

## Material Properties

# Influence of chlorosulfonated polyethylene network structure on poly(acrylonitrile-styrene-acrylate)/poly( $\alpha$ -methylstyrene-acrylonitrile) blends: Mechanical properties, morphologies, glass transition behavior and heat resistance

Pengfei Zhao <sup>a, b</sup>, Ming Wang <sup>a</sup>, Jun Zhang <sup>a, b, \*</sup><sup>a</sup> College of Materials Science & Engineering, Nanjing Tech University, Nanjing, 210009, China<sup>b</sup> Jiangsu Collaborative Innovation Center for Advanced Inorganic Function Composites, Nanjing, 210009, China

## ARTICLE INFO

## Article history:

Received 29 September 2016

Received in revised form

19 November 2016

Accepted 22 November 2016

Available online 25 November 2016

## Keywords:

Acrylonitrile-styrene-acrylate terpolymer

Chlorosulfonated polyethylene

Heat resistance

Network structure

Toughening modification

## ABSTRACT

Acrylonitrile-styrene-acrylate terpolymer and poly( $\alpha$ -methylstyrene-acrylonitrile) (ASA/ $\alpha$ -MSAN, 25/75) with different loadings of chlorosulfonated polyethylene (CSM) were prepared via melt blending, with goals of toughening modification of ASA/ $\alpha$ -MSAN blends and maintaining the heat resistance simultaneously. The results revealed CSM had excellent toughening effect at room temperature. At 0 °C, impact strength increased linearly with CSM content. However, toughening effect of CSM was undesirable at -30 °C. The temperature-dependent toughening efficiency of CSM was significantly related to its glass transition behavior. Scanning electron microscope analysis on cryo-fractured surfaces revealed the toughening mechanism was the formation of CSM toughening network in matrix, which was further confirmed by selective extraction tests. The formation of CSM network could lead to increased glass transition temperature of the blends at the low temperature region according to dynamic mechanical thermal analysis. Different from other toughening agents, CSM network uncompromised the heat resistance of ASA/ $\alpha$ -MSAN blends.

© 2016 Elsevier Ltd. All rights reserved.

## 1. Introduction

The method of polymer blending is an effective and economical way to develop new materials with desirable physical and mechanical properties through simple process technology [1,2]. Toughening modification of brittleness of polymers, based on blending method, has become an important issue in polymer science.

Acrylonitrile-styrene-acrylate (ASA) is a kind of terpolymer with core-shell structure. Poly(butyl-acrylate) (PBA) constituted the elastomer core in ASA, while styrene and acrylonitrile monomers were grafted onto the core to form the rigid styrene-co-acrylonitrile (SAN) shell [3]. ASA has a similar structure with acrylonitrile-butadiene-styrene terpolymer (ABS) and retains almost all the outstanding properties, such as desirable impact

resistance, easy processing properties, chemical resistance, dimensional stability, etc. [4,5] The significant difference between these two kinds of polymer is that the core component of ABS is butadiene rubber with unsaturated main chain, while the core component of ASA is acrylate rubber with saturated main chain. Polymers containing C=C double bonds in main chain are highly susceptible to degradation, which leads to poor weather resistance against UV and heat [6,7]. This significant difference makes ASA more attractive than ABS in long-term outdoor application.

Commercial ASA resin was prepared by combing core-shell ASA terpolymer with SAN in a certain proportion. Although ASA resin has a lot of advantages, the heat-resistance of ASA resin is still poor, which restricts its application in high temperature environment. SAN, the shell phase of ASA terpolymer, was often used to modify the heat resistance of ASA resin. However, the improvement in heat resistance is limited based on previous report. With addition of 50 wt% SAN, the heat distortion temperature (HDT) of the ASA/SAN blends only increased by 5 °C compared to neat ASA resin (measured under a maximum bending stress of 1.80 MPa) [8]. To better modify the poor heat resistance,  $\alpha$ -methylstyrene-

\* Corresponding author. College of Materials Science & Engineering, Nanjing Tech University, Nanjing, 210009, China.

E-mail address: [zhangjun@njtech.edu.cn](mailto:zhangjun@njtech.edu.cn) (J. Zhang).

acrylonitrile copolymer ( $\alpha$ -MSAN) was chosen to blend with ASA resin. The chain of  $\alpha$ -MSAN is more rigid than SAN due to the steric effect caused by the additional methyl group ( $-\text{CH}_3$ ) at its side chain. According to previous study [9], by combining 70 wt%  $\alpha$ -MSAN, the HDT of ASA/ $\alpha$ -MSAN blends could be increased by nearly 20 °C compared to neat ASA resin (measured under a maximum bending stress of 1.80 MPa), indicating that  $\alpha$ -MSAN has a great potential in replacing SAN to modify the heat-resistance of ASA resin. However, the improvement in heat resistance was accompanied with large loss in toughness. As reported, the notched Izod impact strength dropped from 25 kJ/m<sup>2</sup> for neat ASA resin to less than 5 kJ/m<sup>2</sup> for ASA/ $\alpha$ -MSAN (30/70) blends [9]. Therefore, it is essential to explore appropriate toughening agents to enhance the toughness of ASA/ $\alpha$ -MSAN blends. However, introduction of elastomer into a brittle matrix usually lowers the heat resistance. In our previous work, although thermoplastic polyurethane elastomer (TPU) has been successfully used to toughen the ASA/ $\alpha$ -MSAN (25/75) blends [10], the heat resistance of the blends was significantly weakened. Therefore, it is also noteworthy to maintain the heat resistance when a toughening agent is applied in a polymer matrix.

Chlorosulfonated polyethylene (CSM) is a kind of amorphous thermoplastic polymer, comprising a modified polyethylene backbone with chloro and sulfonyl chloride side groups [11,12], which break the regularity and crystalline of polyethylene, thus endowing CSM with high elasticity. In addition, the polar side groups make CSM have good compatibility with a polar matrix of ASA/ $\alpha$ -MSAN. Owing to highly saturated chemical structure compared with other common rubbers, CSM has good properties of weathering, heat aging and ozone resistance [13–15], leading to its widespread use in manufacturing tubes, wire covers, building materials and so on [16]. Although many papers have paid attention to the composites containing CSM elastomer [14,17,18], to best of our knowledge, there is few research concerned about CSM used for toughening modification. Herein, CSM was chosen to toughen ASA/ $\alpha$ -MSAN (25/75) via melt blending. The main purpose of this study is to identify the optimum contents of CSM to be introduced into ASA/ $\alpha$ -MSAN blends, which can enhance the toughness and keep the heat resistance simultaneously. Notched Izod impact test was performed over a wide range of temperatures (25 °C, 0 °C and –30 °C) to evaluate the toughening effect of CSM. The morphologies of cryo-fractured surfaces and impact-fractured surfaces were observed by scanning electron microscopy (SEM). In particular, cryo-fractured surfaces of ASA/ $\alpha$ -MSAN/TPU blends were also observed, in order to compare the difference of toughening mechanism of CSM and TPU. Other mechanical properties, i.e., tensile and flexural properties, were also characterized. Dynamic mechanical thermal analysis (DMTA) was used to study the glass transition behavior of the blends. Heat resistance of the blends was evaluated by Vicat/HDT equipment.

## 2. Experiment

### 2.1. Materials

ASA (Grade: HX-960) copolymer, 60 wt% PBA content, was friendly supplied by Zibo Huaxing additives Co., Ltd., China.  $\alpha$ -MSAN (Grade: NR-188) containing 30 wt% of acrylonitrile was procured from Yixin Lilai Chemical Co., Ltd., China. CSM (Grade: CSM-3304) with 35 wt% chlorine content and 1 wt% sulfur content was manufactured by PetroChina Jilin Petrochemical Co., Ltd., China.

### 2.2. Sample preparation

The ASA/ $\alpha$ -MSAN/CSM blends with different weight ratios of 25/

75/0, 25/75/5, 25/75/10, 25/75/15, 25/75/20 and 25/75/30 were prepared through melt blending at 180 °C, using a two-roll mill. 0.5 phr anti-oxidant was used to avoid thermal degradation during the blending process. 0.5 phr polyethylene wax and 0.5 phr calcium stearate were added to improve the processability. The obtained polymer blends were subsequently processed into sheets of approximately 2 mm and 4 mm in thickness by compression-molding, using a flat plate vulcanization machine, at 180 °C for 15 min under a 10 MPa pressure. The dumb-bell shaped pieces with 2 mm thickness for tensile tests were cut from the sheets with a die. Rectangular samples with a dimension of 80 × 10 × 4 mm<sup>3</sup> were also machined from the sheets, used for flexural, impact and HDT tests.

### 2.3. Characterization

#### 2.3.1. Mechanical properties measurements

The notched Izod impact strength tests were carried out on an Izod impact tester (UJ-4, Chengde Machine Factory, China). In order to evaluate the toughness of the blends at different temperatures. The prepared samples were preserved at –30 °C, 0 °C and 25 °C for 12 h prior to the impact test. Tensile and flexural properties of the blends were measured through a universal testing machine (CMT 5254, Shenzhen SANS Testing Machine Co., Ltd., China). The tests were carried out at crosshead speeds of 5 mm/min for tensile tests (ISO 527) and 2 mm/min for flexural tests (ISO 178), respectively. At least three specimens were tested for each polymer system and the mean values were calculated.

#### 2.3.2. Scanning electron microscope analysis

The morphologies of cryo-fractured surfaces (using liquid nitrogen) and impact-fractured surfaces of the blends were observed by scanning electron microscope (JSM-5900, JEOL Ltd., Japan), with an accelerating voltage of 15 kV. All the fractured surfaces of blends were coated with a thin conductive layer of gold before viewing.

#### 2.3.3. Selective extraction tests

Each specimen cut from sheets of 2 mm thickness was immersed with acetone for 4 days at room temperature without stirring. Acetone was selected because it is a good solvent for  $\alpha$ -MSAN, but a poor solvent for CSM, TPU and ASA.

#### 2.3.4. Dynamic mechanical thermal analysis

The glass transition behavior of ASA/ $\alpha$ -MSAN/CSM blends was characterized by a dynamic mechanical thermal analyzer (MCR302, Anton Paar GmbH, Austria). The dimension of samples prepared for testing was approximately 25 × 6 × 2 mm<sup>3</sup>. The experiment was carried from –90 °C to 160 °C at a heating rate of 3 °C/min, with a fixed torsional frequency of 1 Hz.

#### 2.3.5. Heat distortion temperature measurements

The HDT of the ASA/ $\alpha$ -MSAN/CSM blends was tested by the Vicat/HDT equipment (ZWK1302-2, Shenzhen SANS Testing Machine Co., Ltd., China) with a heating rate of 120 °C/h. The HDT was measured under a three-point bending stress of 1.80 MPa and 0.45 MPa, respectively, according to ISO 75-1.

## 3. Results and discussion

### 3.1. Mechanical properties

Fig. 1 shows the impact strength of ASA/ $\alpha$ -MSAN/CSM ternary blends at three different temperatures (25 °C, 0 °C and –30 °C). It can be observed that the impact strength increases with CSM content at 25 °C and 0 °C. At room temperature, the impact strength

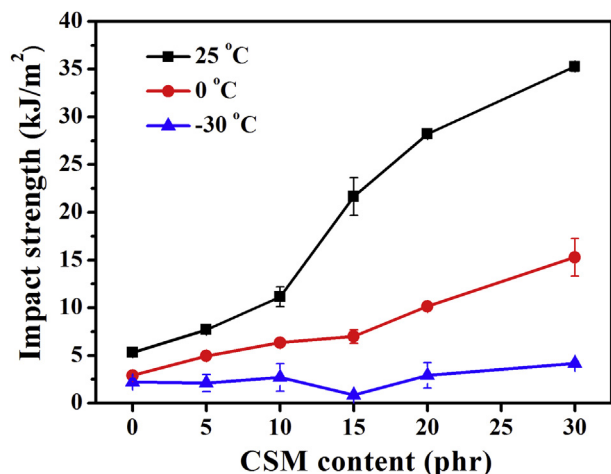


Fig. 1. Impact strength of ASA/α-MSAN/CSM (27/75/0-30) ternary blends at different temperatures.

increases dramatically from 5.3 kJ/m<sup>2</sup> for pristine ASA/α-MSAN (25/75) to 35.3 kJ/m<sup>2</sup> for ASA/α-MSAN/CSM (25/75/30). A sharp brittle-ductile transition appears in the curve at 25 °C when the CSM content increases from 10 phr to 20 phr, the failure mode of tested samples changes from brittle fracture (11.2 kJ/m<sup>2</sup>) to ductile fracture (28.2 kJ/m<sup>2</sup>). It can also be observed that the rising slope of impact strength from 20 phr to 30 phr is relatively smaller than that from 10 phr to 20 phr.

Different from the obvious brittle-ductile transition in the curve at 25 °C, impact strength increases linearly with CSM content at 0 °C. The value of impact strength increases from 2.9 kJ/m<sup>2</sup> for ASA/α-MSAN (25/75) to 15.3 kJ/m<sup>2</sup> for ASA/α-MSAN/CSM (25/75/30). However, CSM loses the toughening effect at -30 °C, all the samples exhibit brittle behavior and the impact strength is kept lower than 5 kJ/m<sup>2</sup>. In conclusion, incorporation of CSM can enhance the toughness of ASA/α-MSAN at 25 °C and 0 °C, whereas no toughening effect is observed at -30 °C. The temperature dependence of toughening effect is likely related to glass transition temperature ( $T_g$ ) of CSM, which will be discussed in detail in the following part.

Fig. 2 shows the effect of CSM content on tensile properties of ASA/α-MSAN/CSM. Noted that the tensile strength decreases linearly with CSM content. The value of tensile strength drops from 40.1 MPa to 29.7 MPa with addition of 30 phr CSM. However, the retention ratio of tensile strength is still 86% for ASA/α-MSAN/CSM (25/75/20) (34.6 MPa). Elongation at break is usually used to

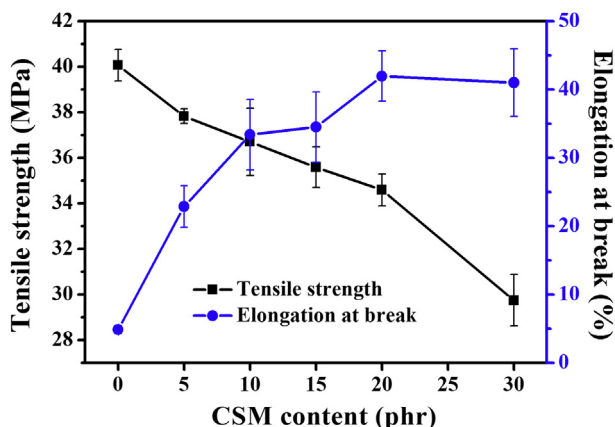


Fig. 2. Tensile properties of ASA/α-MSAN/CSM (27/75/0-30) ternary blends.

characterize the toughness of materials, and it parallels the impact strength well as shown in Fig. 1. The ASA/α-MSAN (25/75) binary blends is brittle with elongation at break of only 5%. With addition of 20 phr CSM, the elongation at break can be increased to 42%. However, the addition of 30 phr CSM doesn't lead to further growth in elongation at break, which is similar to impact strength. It can be concluded from tensile test that ASA/α-MSAN/CSM blends obtain high elongation at break and retention of tensile strength with addition of 20 phr CSM.

With regard to flexural properties (Fig. 3), both flexural strength and flexural modulus exhibit almost the same variation trend and decrease with CSM content. With addition of CSM from 0 phr to 30 phr, flexural strength of the blends decreases from 68.5 MPa to 40.1 MPa, while the modulus decreases from 2547 MPa to 1445 MPa. Flexural properties are generally used to characterize the stiffness of materials. In this study, the increased CSM content in ASA/α-MSAN matrix leads to the decrement of stiffness.

### 3.2. SEM analysis

The morphologies of cryo-fractured surfaces were observed by SEM shown in Fig. 4. In order to compare the toughening mechanism of CSM and TPU, the cryo-fractured morphologies of ASA/α-MSAN/CSM and ASA/α-MSAN/TPU were both investigated. It should be noted that the ASA/α-MSAN/TPU (25/75/10, 20, 30) blends were completely same as the blends prepared in our previous report [10]. Many holes can be observed in Fig. 4a, which is attributed to the cavitation of ASA core-shell particles. It can be found that ASA core-shell particles can keep the spherical shape after melt blending and disperse well in the matrix. With respect to ASA/α-MSAN/CSM blends (Fig. 4b–d), besides cavitation holes, thread-like substances appear and tend to form a network structure in the matrix with the increase in the CSM content. Considering the CSM content as the sole variable in ASA/α-MSAN, these thread-like substances were inevitable to be CSM. Therefore, the toughening mechanism can be determined as the formation of CSM toughening network, which is similar to the chlorinated polyethylene (CPE) [19]. With increasing content, the discrete CSM can gradually form a continuous network structure in the brittle matrix. Once the blends are under impact load, the network will transfer, disperse, and absorb the impact energy, which can avoid appearance of local stress concentration. In addition, large amounts of crazes and shear bands will be induced by large deformation of CSM elastomer, giving rise to excellent improvement in toughness.

In stark contrast, only cavitation holes can be observed from the cryo-fractured surfaces of ASA/α-MSAN/TPU (25/75/10-30) blends

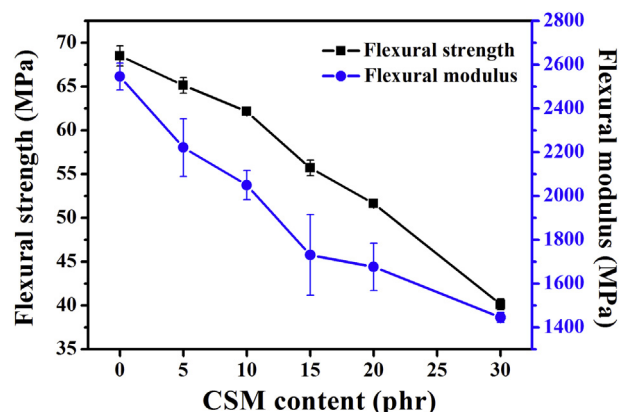


Fig. 3. Flexural properties of ASA/α-MSAN/CSM (27/75/0-30) ternary blends.

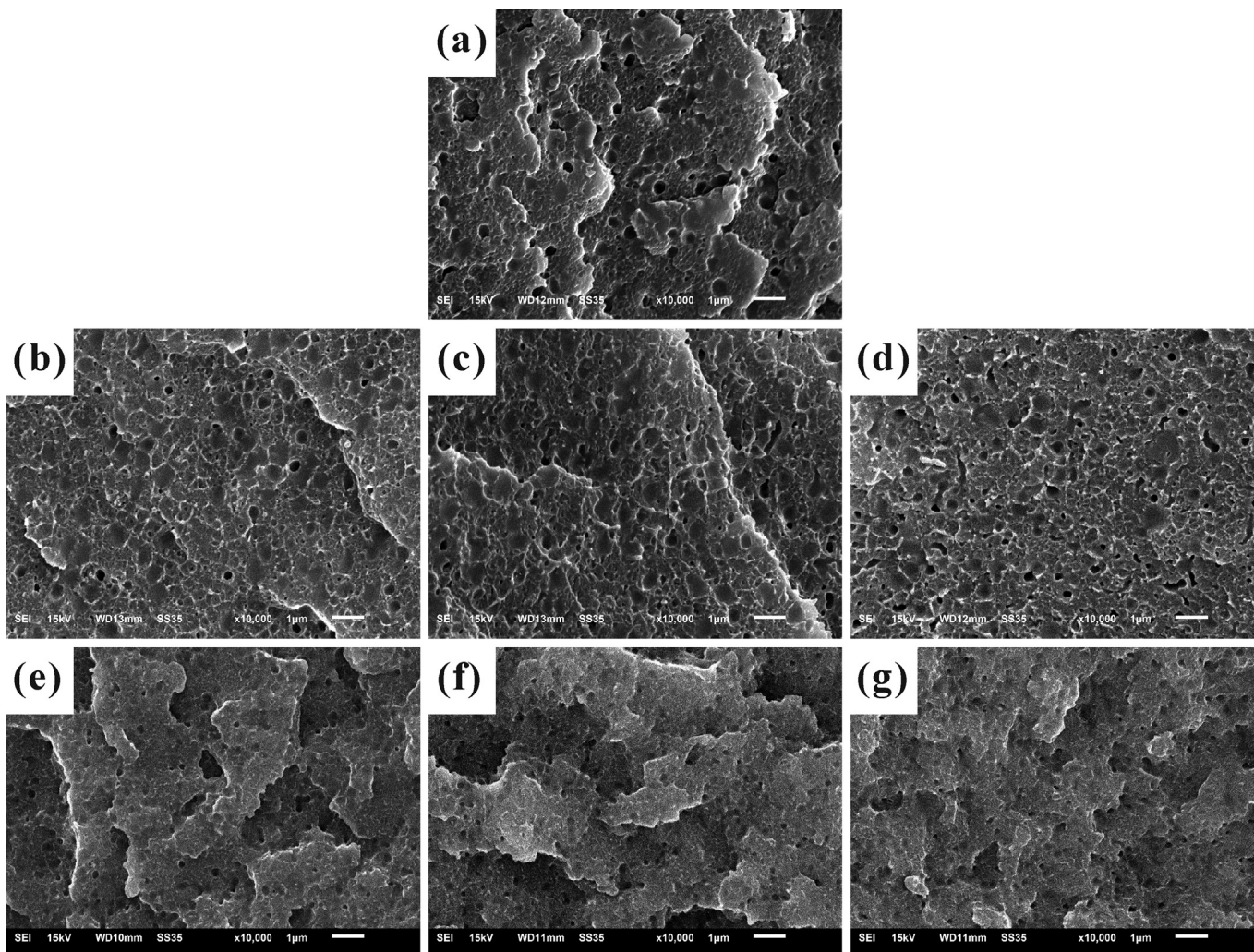
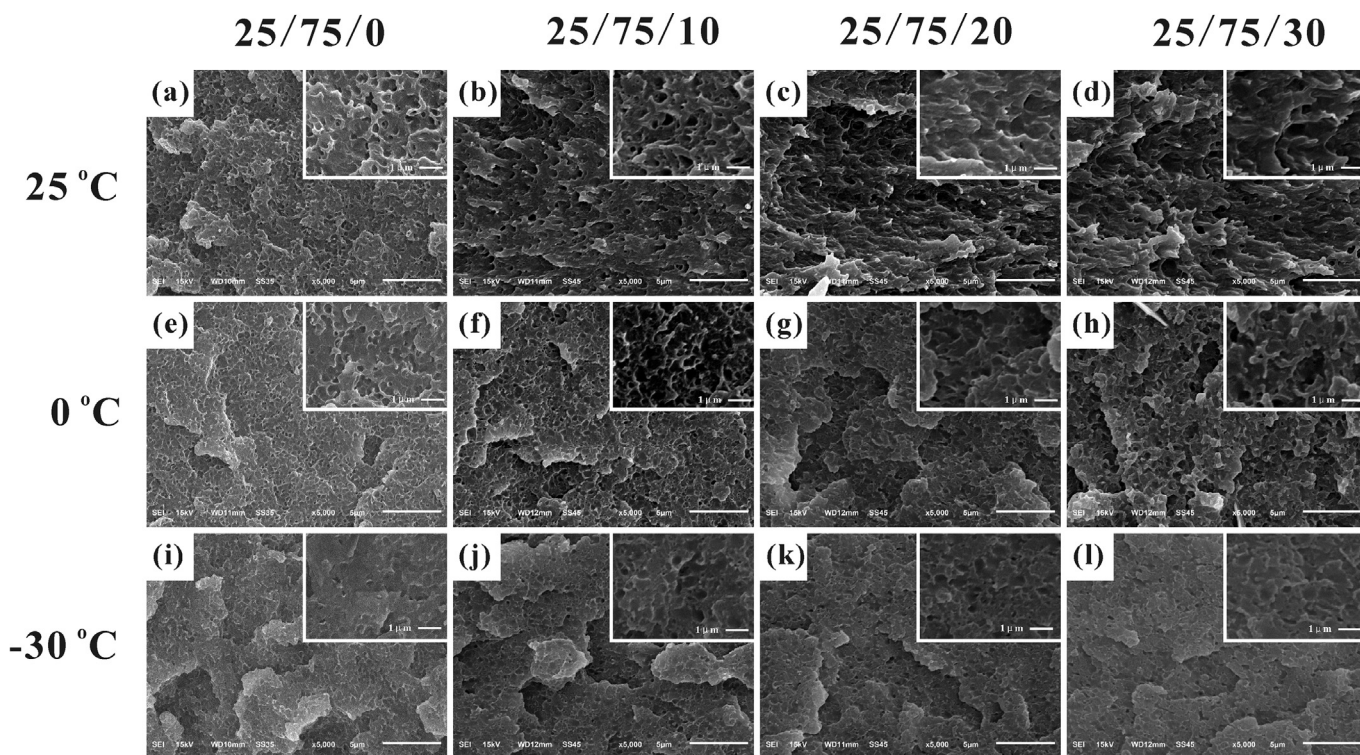


Fig. 4. Cryo-fractured morphologies of (a): ASA/ $\alpha$ -MSAN (25/75), (b)–(d): ASA/ $\alpha$ -MSAN/CSM (25/75/10, 20, 30) and (e)–(g): ASA/ $\alpha$ -MSAN/TPU (25/75/10, 20, 30).

(Fig. 4e–g), and no thread-like network structure can be found. It indicates that the TPU only dispersed in the ASA/ $\alpha$ -MSAN matrix in the form of particles. Cavitation is the main toughening mechanism of ASA/ $\alpha$ -MSAN/TPU blends. According to experimental data from our previous report [10], with addition of 10 phr, 20 phr, and 30 phr TPU, the notched Izod impact strength at room temperature of ASA/ $\alpha$ -MSAN/TPU blends was 11.34 kJ/m<sup>2</sup>, 21.93 kJ/m<sup>2</sup>, and 26.51 kJ/m<sup>2</sup>, respectively. Herein, with addition of 10 phr, 20 phr, and 30 phr CSM, the notched Izod impact strength at room temperature of ASA/ $\alpha$ -MSAN/CSM blends was 11.15 kJ/m<sup>2</sup>, 28.21 kJ/m<sup>2</sup>, and 35.28 kJ/m<sup>2</sup>, respectively. Comparatively speaking, CSM has higher efficiency than TPU at room temperature, which means the toughening network mechanism is superior to cavitation mechanism for toughening ASA/ $\alpha$ -MSAN at room temperature. It is interesting to note that the ASA/ $\alpha$ -MSAN/TPU (25/75/10) blend and the ASA/ $\alpha$ -MSAN/CSM (25/75/10) blend still show a similar impact strength of approximately 11 kJ/m<sup>2</sup>. However, when 20 phr toughening agent is added, the difference of toughening efficiency appears. It can be speculated that 10 phr CSM is not enough to form the complete toughening network because of its low content. Therefore, CSM has similar toughening effect like TPU. However, when the CSM content is high enough to form the complete toughening network, CSM shows a higher toughening efficiency than TPU when the same content of toughening agent was added.

SEM analysis was also used to observe the morphologies of impact-fractured surfaces of the ASA/ $\alpha$ -MSAN/CSM blends. At 25 °C, ASA/ $\alpha$ -MSAN (25/75) (Fig. 5a) exhibits a relatively smooth and flat impact-fractured surface. In a higher magnification, many small holes can be seen in the matrix, which is attributed to the cavitation of ASA core-shell particles after impact fracture. With addition of 10 phr CSM, the ASA/ $\alpha$ -MSAN/CSM (25/75/10) blend shows an obvious oriented morphology (Fig. 5b), and the impact-fractured surface becomes rougher. Generally, polymer materials with rougher impact-fractured surfaces own higher toughness. Based on the variation of the impact-fractured surface, the toughness of blends actually becomes higher by incorporating 10 phr CSM. With addition of 20 phr and 30 phr CSM, the impact-fractured surfaces exhibit deeper level of oriented morphologies (Fig. 5c and d). The change in morphologies explains the transition of toughening mechanism. For ASA/ $\alpha$ -MSAN (25/75) blend without CSM, the toughening behavior is mainly attributed to the cavitation of ASA core-shell particles. However, when the CSM network is formed in the matrix, the toughening network will undergo large deformation to share and transfer the impact load, thus causing oriented morphologies after impacting. According to the changing degree of impact-fractured surfaces, the rudiment of CSM network is preliminarily formed with addition of 10 phr CSM, and becomes complete with addition of 20 phr and 30 phr CSM. In addition, the



**Fig. 5.** SEM micrographs of impact-fractured surfaces of ASA/ $\alpha$ -MSAN/CSM (27/75/0, 10, 20, 30) ternary blends, (a)–(d): impact at 25 °C, (e)–(h): impact at 0 °C, (i)–(l): impact at –30 °C.

surfaces of Fig. 5c and d also become rougher compared with that of Fig. 5b. The apparent morphology transition from ASA/ $\alpha$ -MSAN/CSM (25/75/10) to ASA/ $\alpha$ -MSAN/CSM (25/75/20) also agrees well with the brittle–ductile transition observed in notched Izod impact test at 25 °C. It can be confirmed that the CSM toughening network is completely formed with addition of 20 phr CSM. Since 20 phr CSM is enough to constitute the toughening network, the further addition of 30 phr CSM will not lead to substantial increase in impact strength or elongation at break.

When impacted at 0 °C, the impact-fractured surfaces show no obvious change. Fractured surfaces gradually become rougher with increasing CSM content (Fig. 5e–h). However, none of the samples shows the morphology of ductile fracture, which is also in accordance with the results of impact tests that the impact strength increased linearly at 0 °C without an apparent brittle–ductile transition. With respect to SEM graphs of –30 °C, all the observed impact-fractured surfaces show the flat morphologies (Fig. 5i–l), indicating brittle fracture of all the tested samples.

In conclusion, the morphologies of impact-fractured surfaces observed by SEM are in good agreement with the results of impact test. SEM analysis establishes the relationship between mechanical properties and microstructure of the blends.

### 3.3. The verification of CSM network

Zhen Zhang et al. [20] used the method of selective extraction to prove the existence of CPE network structure in ASA. In this study, this method was also adopted to further prove the formation of network structure by addition of CSM. As shown in Fig. 6, the tested samples cut from sheets with 2 mm thickness were immersed in acetone for 4 days at room temperature. For comparison, both ASA/ $\alpha$ -MSAN/CSM and ASA/ $\alpha$ -MSAN/TPU blends were tested. It is known that acetone is good solvent for  $\alpha$ -MSAN, but a poor solvent

for ASA, CSM and TPU at room temperature. As shown in Fig. 6a, the continuous phase,  $\alpha$ -MSAN, in ASA/ $\alpha$ -MSAN (25/75) was dissolved by acetone and the tested sample was broken apart, the white precipitate at the bottom is the insoluble ASA. In contrast, the ASA/ $\alpha$ -MSAN/CSM blends, even only with addition of 10 phr CSM, cannot be dissolved in acetone after immersed for 4 days (Fig. 6b, c and d). However, all the ASA/ $\alpha$ -MSAN/TPU blends were broken apart in the acetone for 4 days immersion (Fig. 6e, f and g). Based on the fact that ASA, TPU and CSM are all insoluble in acetone, the reason for this change is that CSM can form a continuous network in matrix, which can prevent  $\alpha$ -MSAN from being dissolved and broken apart in acetone. However, both ASA and TPU disperse in  $\alpha$ -MSAN in the form of individual particles, which cannot protect the continuous  $\alpha$ -MSAN phase from being dissolved.

### 3.4. DMTA analysis

The DMTA results of different samples are given in Fig. 7. The  $\tan \delta$  vs. temperature curves of ASA/ $\alpha$ -MSAN/CSM ternary blends exhibit three distinct damping peaks. As shown in Table 1,  $T_{g,1}$  and  $T_{g,2}$  correspond to the glass transition of PBA core of ASA and CSM, respectively. As the shell phase of ASA, SAN has  $T_{g,3}$  at 119 °C. However, in this study,  $\alpha$ -MSAN is the major component which constitutes the continuous phase, and the damping peak of SAN is thus covered by  $T_{g,4}$  of  $\alpha$ -MSAN with stronger intensity.

The temperature-dependent toughening efficiency of CSM can be explained by its  $T_g$ . It can be found in Table 1 that the  $T_g$  of CSM locates in the range of –19.8 °C ~ –5.4 °C. At 25 °C and 0 °C, the temperature is above  $T_g$ , CSM network is kept in a high elastic state. Therefore, toughness of blends can be improved by CSM. When the test temperature drops to –30 °C, the chain segments of CSM are completely frozen, thus resulting in that CSM network at glassy state is ineffective in toughening ASA/ $\alpha$ -MSAN.

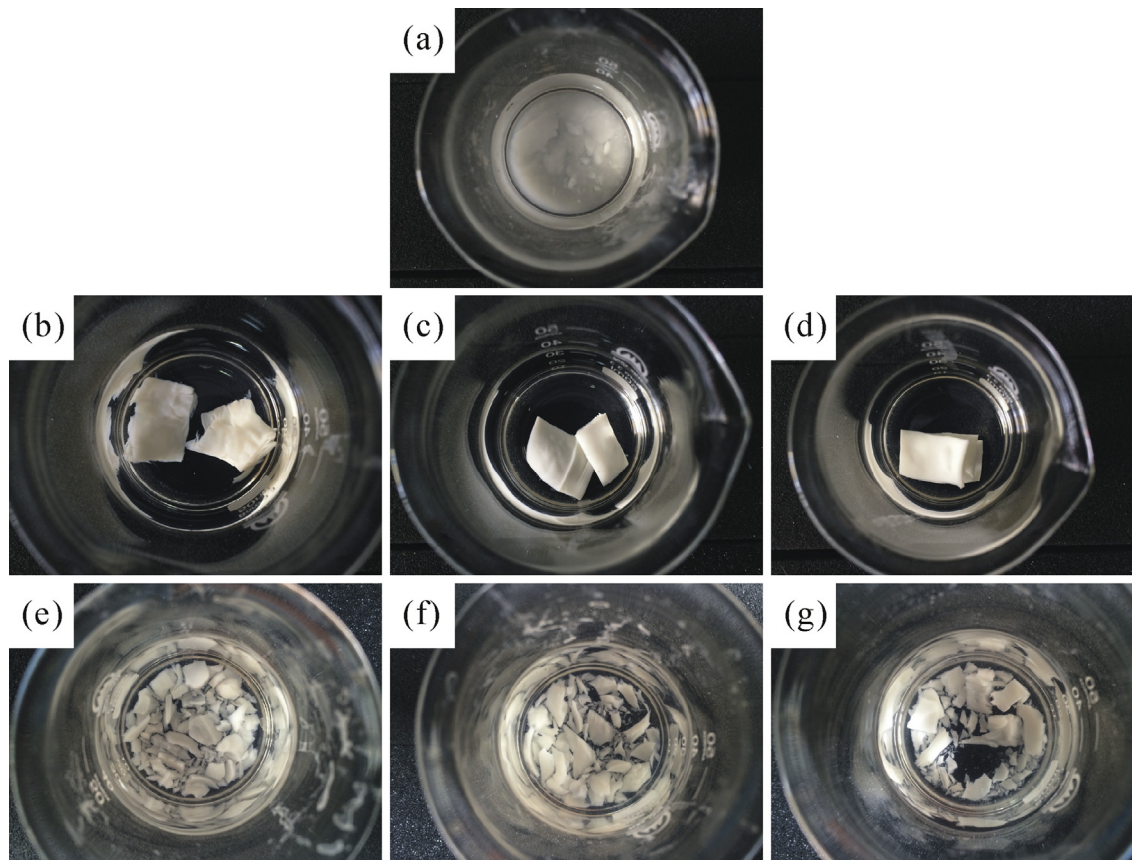


Fig. 6. Images of blends immersed in acetone for 4 days (a): ASA/ $\alpha$ -MSAN (25/75), (b)-(d): ASA/ $\alpha$ -MSAN/CSM (25/75/10, 20, 30), (e)-(g): ASA/ $\alpha$ -MSAN/TPU (25/75/10, 20, 30).

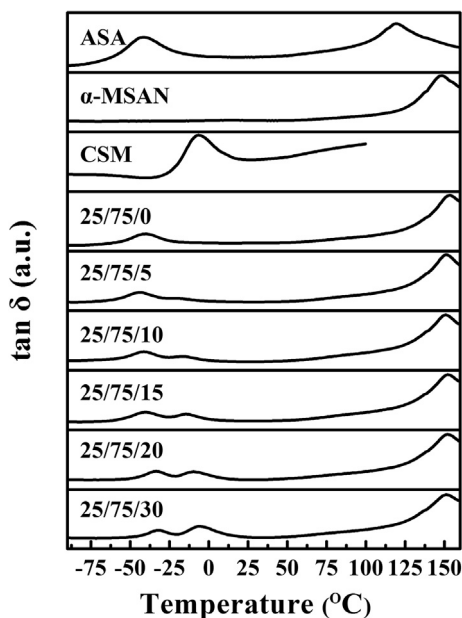


Fig. 7.  $\tan \delta$  curves for ASA,  $\alpha$ -MSAN, CSM and ASA/ $\alpha$ -MSAN/CSM ternary blends (25/75/0-30) with different blend ratios.

Specifically, the  $T_{g,1}$  of PBA is around  $-40$  °C with addition of 0–15 phr CSM. Further addition of 20 phr and 30 phr leads to a sharp increase in  $T_{g,1}$  to about  $-33$  °C. Similar transition is also observed in  $T_{g,2}$  of CSM.  $T_{g,2}$  exhibits a rising trend from  $-19.8$  °C

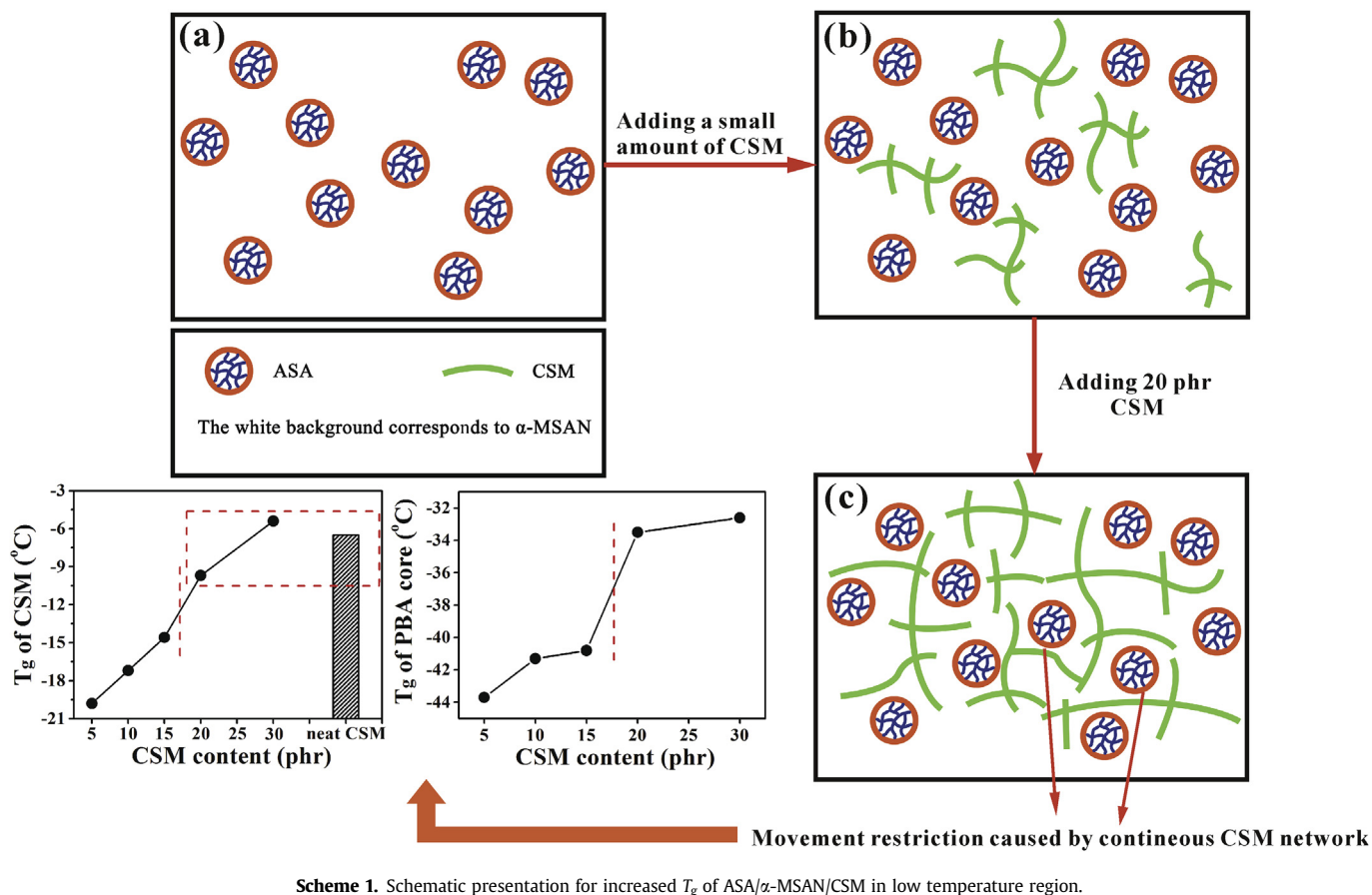
to  $-5.4$  °C, and the sharp change-point also appears when the addition of CSM is 20 phr. As shown in Scheme 1, the gradually increased  $T_g$  of ternary blends in the low temperature region is attributed to the formation of CSM network. When the network was formed, the CSM phase in blends changed from a separate phase (Scheme 1b) to a continuous phase (Scheme 1c), and the  $T_{g,2}$  of CSM also varied to the  $T_g$  of neat CSM.  $T_{g,2}$  of ASA/ $\alpha$ -MSAN/CSM (25/75/20) and ASA/ $\alpha$ -MSAN/CSM (25/75/30) blends is  $-9.7$  °C and  $-5.4$  °C, respectively, which is close to the  $T_g$  of neat CSM ( $-6.5$  °C). This means the continuous network structure is formed in matrix with addition of 20 phr and 30 phr CSM, which corresponds to the results discussed above. The change of  $T_{g,1}$  of PBA core is also ascribed to the CSM network. Below  $-30$  °C,  $T_{g,1}$  shows an increasing trend because the CSM network at glassy state may restrict the movement of ASA particles (Scheme 1c). The restriction effect becomes strongest when the CSM network is completely formed. Therefore, addition of 20 phr CSM leads to a sudden rise in  $T_{g,1}$  of PBA.

The variation of  $T_g$  also has significant influence on toughness of the blends at 0 °C and  $-30$  °C. According to the results of impact tests, the impact strength at 0 °C increases linearly but shows no brittle-ductile transition, and the impact strength at  $-30$  °C is below  $5$  kJ/m<sup>2</sup>. Although the CSM content increases, the  $T_g$  of PBA core and CSM also rises to approximately  $-30$  °C and 0 °C, respectively. In other words, chain flexibility of PBA and CSM was gradually weakened at low temperature when CSM content increases. Therefore, even with addition of 20 phr or 30 phr CSM, the toughening effect is still not remarkable at low temperature, and the brittle-ductile transition is difficult to happen.

The analysis on the glass transition behavior gives a possible

**Table 1**  
Storage modulus (25 °C) and  $T_g$  values of ASA/ $\alpha$ -MSAN/CSM blends obtained from DMTA tests.

ASA/ $\alpha$ -MSAN/CSM	Storage modulus (Pa)	$T_{g,1}$ (°C)	$T_{g,2}$ (°C)	$T_{g,3}$ (°C)	$T_{g,4}$ (°C)
100/0/0	$1.29 \times 10^8$	-41.9	–	119	–
0/100/0	$3.47 \times 10^9$	–	–	–	148
0/0/100	$5.12 \times 10^6$	–	-6.5	–	–
25/75/0	$2.58 \times 10^9$	-39.9	–	–	153
25/75/5	$2.50 \times 10^9$	-43.7	-19.8	–	151
25/75/10	$2.27 \times 10^9$	-41.3	-17.2	–	151
25/75/15	$2.05 \times 10^9$	-40.8	-14.6	–	152
25/75/20	$2.13 \times 10^9$	-33.5	-9.7	–	152
25/75/30	$1.47 \times 10^9$	-32.6	-5.4	–	151



explanation on the temperature-dependent toughening efficiency of CSM, and agrees well with the result that the complete toughening network can be formed with addition of 20 phr CSM.

Storage modulus is representative of stiffness of materials. As shown in Fig. 8 and Table 1, storage modulus of ASA increases by an order of magnitude after blending with  $\alpha$ -MSAN (from  $1.29 \times 10^8$  Pa to  $2.58 \times 10^9$  Pa). Meanwhile, the ASA/ $\alpha$ -MSAN blends can retain a high storage modulus and keep almost unchanged until 125 °C. This suggests that the introduction of  $\alpha$ -MSAN can simultaneously enhance stiffness and heat resistance of ASA. With addition of 0 phr–30 phr CSM, the storage modulus shows a slight decrement, which is in accordance with the decreased flexural strength and modulus. The temperature that storage modulus shows significant variation is around 125 °C, and no obvious change is found with increasing CSM content, which means that CSM only has a slight effect on the soft temperature of ASA/ $\alpha$ -MSAN blend.

### 3.5. Heat distortion temperature analysis

Heat resistance is a valuable property of ASA/ $\alpha$ -MSAN blends. When it is toughened by a kind of elastomer, it is important to keep the heat resistance uncompromised. Heat distortion temperature is the most direct presence of heat resistance. As shown in Fig. 9, the HDT of ASA/ $\alpha$ -MSAN/CSM blends shows no obvious change and keeps at a high level around 115 °C even with addition of 20 phr CSM (measured under a maximum bending stress of 0.45 MPa). When measured under a maximum bending stress of 1.80 MPa, the HDT shows a slight decline with the CSM content, the value decreases from 104 °C for ASA/ $\alpha$ -MSAN to 100 °C for blend with 20 phr CSM. Only the blend containing 30 phr CSM shows an apparent decline in HDT. It can be concluded that blending less than 20 phr CSM with ASA/ $\alpha$ -MSAN only slightly sacrifices the heat resistance. The results of HDT tests are in agreement with the thermo-mechanical properties measured in DMTA tests. In our

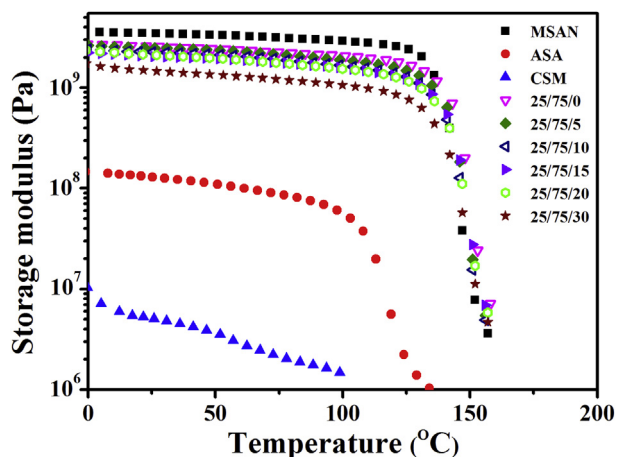


Fig. 8. Variation in storage modulus of ASA,  $\alpha$ -MSAN, CSM and ASA/ $\alpha$ -MSAN/CSM ternary blends (25/75/0-30) with different blend ratios.

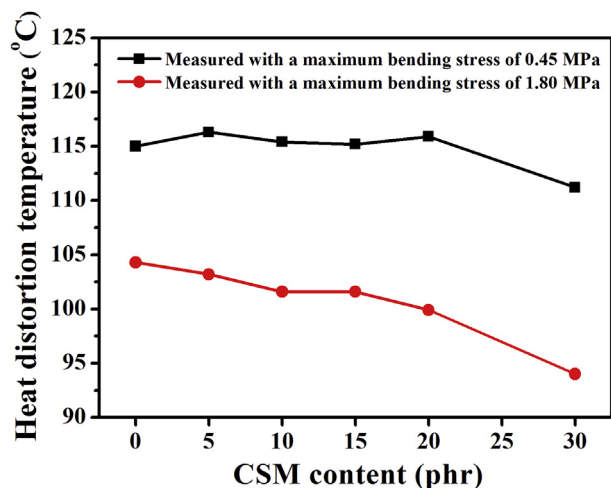


Fig. 9. Heat resistance of ASA/ $\alpha$ -MSAN/CSM (27/75/0-30) ternary blends.

previous report [10], with addition of 20 phr TPU, the HDT of ASA/ $\alpha$ -MSAN (25/75) decreased by 6 °C and 12 °C, measured under a maximum bending stress of 0.45 MPa and 1.80 MPa, respectively. It reveals that CSM is superior to TPU in terms of keeping the heat resistance of ASA/ $\alpha$ -MSAN.

As is well known, introducing rubber phase with poor heat resistance to polymer matrix can lower the HDT of blends. Herein, CSM has no obvious negative influence on heat resistance because of the network structure formed in the matrix that can sustain and share the bending load in HDT tests. Therefore, the structure of the ASA/ $\alpha$ -MSAN/CSM samples is relatively stable when heated.

#### 4. Conclusion

In this study, CSM was introduced to ASA/ $\alpha$ -MSAN blend to modify the brittleness. Notched Izod impact tests showed CSM could greatly enhance the toughness of the blends at room temperature. The obvious brittle-ductile transition appeared in the range of 10 phr–20 phr CSM. At 0 °C, the impact strength increased linearly with CSM content, whereas CSM lost the toughening effect at –30 °C. SEM analysis on cryo-fractured surfaces and selective extraction tests proved the formation of CSM toughening network in ASA/ $\alpha$ -MSAN matrix. It was also found that 20 phr CSM was

needed to form the complete toughening network. By forming the toughening network, CSM showed higher toughening effect than TPU at room temperature.

The formation of CSM network led to increased  $T_g$  for ternary blends at the low temperature region. By adding 5 phr–30 phr CSM,  $T_g$  of PBA and CSM increased from –43.7 °C to –32.6 °C and –19.8 °C to –5.4 °C, respectively. The  $T_g$  of CSM in ternary blends located in the range of –20 °C ~ –5 °C, which caused the temperature dependence of CSM's toughening efficiency in the notched Izod impact tests. Based on the results of storage modulus and HDT tests, addition of CSM only slightly sacrificed the heat resistance of ASA/ $\alpha$ -MSAN because of the existence of network structure. HDT of the ternary blends kept almost unchanged even with addition of 20 phr CSM. With respect to the tensile and flexural properties, tensile strength, flexural strength, and flexural modulus decreased with the CSM content. Elongation at break increased significantly from 5% to 42% with addition of 20 phr CSM. Considering all the factors, the blending weight ratio of ASA/ $\alpha$ -MSAN/CSM was determined to be 25/75/20, which reached the best comprehensive performance.

#### Acknowledgements

This work was supported by the Priority Academic Program Development of Jiangsu Higher Education Institutions (PAPD).

#### References

- [1] J.Q. Xia, J. Zhang, G.X. Liao, X.G. Jian, Copolymerization and blending of poly(phthalazinone ether ketone)s to improve their melt processability, *J. Appl. Polym. Sci.* 103 (4) (2007) 2575.
- [2] J.A. Schmitt, H. Keskkula, Short-time stress relaxation and toughness of rubber-modified polystyrene, *J. Appl. Polym. Sci.* 3 (8) (1960) 132.
- [3] S. Tolue, M.R. Moghbeli, S.M. Ghafelbashi, Preparation of ASA (acrylonitrile-styrene-acrylate) structural latexes via seeded emulsion polymerization, *Eur. Polym. J.* 45 (3) (2009) 714.
- [4] J. An, C. Kim, B.H. Choi, J.M. Lee, Characterization of acrylonitrile-butadiene-styrene (ABS) copolymer blends with foreign polymers using fracture mechanism maps, *Polym. Eng. Sci.* 54 (12) (2014) 2791.
- [5] M.I. Triantou, P.A. Tarantili, Studies on morphology and thermomechanical performance of ABS/PC/organoclay hybrids, *Polym. Compos.* 35 (7) (2014) 1395.
- [6] C.K. Radhakrishnan, R. Alex, G. Unnikrishnan, Thermal, ozone and gamma ageing of styrene butadiene rubber and poly(ethylene-co-vinyl acetate) blends, *Polym. Degrad. Stabil.* 91 (4) (2006) 902.
- [7] M.R. Moghbeli, S. Blue, Acrylonitrile/Styrene/Acrylate structural rubber latex particles as impact modifier for SAN copolymer, *Iran. Polym. J.* 20 (2) (2011) 137.
- [8] W. Zhang, S. Chen, J. Zhang, Influence of blend composition on mechanical properties of ASA/SAN binary blends, *J. Thermoplast. Compos.* 26 (3) (2013) 322.
- [9] W. Zhu, J. Zhang, Mechanical and thermal properties of (acrylonitrile-styrene-acrylic)/( $\alpha$ -methylstyrene-acrylonitrile) binary blends, *J. Vinyl Addit. Technol.* 22 (2) (2016) 156.
- [10] P.F. Zhao, J. Zhang, Room temperature and low temperature toughness improvement in PBA-g-SAN/ $\alpha$ -MSAN by melt blending with TPU, *Rsc Adv.* 6 (19) (2016) 15701.
- [11] Z. Gu, G.J. Song, W.S. Liu, J.M. Gao, W. Dou, P. Lu, Preparation and properties of chlorosulfonated polyethylene/organomontmorillonite nanocomposites, *J. Appl. Polym. Sci.* 115 (6) (2010) 3365.
- [12] K.T. Gillen, R. Assink, R. Bernstein, M. Celina, Condition monitoring methods applied to degradation of chlorosulfonated polyethylene cable jacketing materials, *Polym. Degrad. Stabil.* 91 (6) (2006) 1273.
- [13] Y.J. Tan, J.H. Tang, A.M. Deng, Q. Wu, T.C. Zhang, H.Z. Li, Magnetic properties and microwave absorption properties of chlorosulfonated polyethylene matrices containing graphite and carbonyl-iron powder, *J. Magn. Magn. Mat.* 326 (2013) 41.
- [14] M. Nanda, D.K. Tripathy, Rheological behavior of chlorosulfonated polyethylene composites: effect of filler and plasticizer, *J. Appl. Polym. Sci.* 126 (1) (2012) 46.
- [15] Q.B. Li, M.Y. Liao, Thermal properties of chlorosulfonated polyethylene via gas-solid phase method, *J. Therm. Anal. Calorim.* 117 (3) (2014) 1105.
- [16] T. Naruse, T. Hattori, Y. Yamaguchi, T. Kanai, T. Sekiya, Thermal degradation of chlorosulfonated polyethylene rubber and ethylene propylene diene terpolymer, *Mater. Des.* 42 (2012) 147.
- [17] G. Janowska, A. Kucharska-Jastrzabek, A. Kasiczak, W.M. Rzymiski, Thermal

- properties and combustibility of cross-linked XNBR/CSM blends, *J. Therm. Anal. Calorim.* 104 (3) (2011) 1107.
- [18] X.F. Bai, X.L. He, J. Zhang, X. Zhu, H.Y. Zhang, R.H. Cheng, B.P. Liu, Improvement of interfacial interaction, dispersion, and properties of chlorosulfonated polyethylene/sio2 nanocomposites using CSPE-g-Sio2 nanoparticles synthesized under ultrasonics, *Polym. Compos.* 33 (6) (2012) 940.
- [19] Z. Zhang, S.J. Chen, J. Zhang, B. Li, X.P. Jin, Influence of chlorinated polyethylene on poly (vinyl chloride)/poly (alpha-methylstyrene-acrylonitrile) blends: mechanical properties, morphology and thermal properties, *Polym. Test.* 29 (8) (2010) 995.
- [20] Z. Zhang, S.C. Wang, J. Zhang, W.Q. Zhu, X.J. Zhao, T.S. Tian, T.T. Chen, Self-formation of elastomer network assisted by nano-silicon dioxide particles: a simple and efficient route toward polymer nanocomposites with simultaneous improved toughness and stiffness, *Chem. Eng. J.* 285 (2016) 439.